

Cascaded Output Selection for Processing of Capacitive Electrocardiograms by Means of Independent Component Analysis

Daniel Wedekind, Hagen Malberg and Sebastian Zaunseder

Abstract—Innovative measurement systems allow for the contact-less recording of vital signs. Thus, applications with medical background for daily life become possible. Aquired signals, however, often cannot compete with their clinically established counterparts. In fact, typical characteristics as small signal amplitudes on the one hand, frequently occurring artefacts and noise on the other hand, introduce the apparent need for sophisticated processing techniques to allow for a reliable function when thinking of contact-less measurements. This contribution investigates the possibility of using multichannel capacitive electrocardiogram (cECG) recordings to derive the heart rate for driver monitoring. We propose a processing scheme consisting of a spatio-temporal independent component analysis applied to the cECG together with a newly developed method to select the most appropriate of the output channels by analyzing their frequency characteristics. By an experimental study incorporating 27 healthy subjects we prove the applicability of our method and discuss its advantages compared to existing methods.

Index Terms—automotive, capacitive ECG, cECG, Independent Component Analysis, ICA, raw data fusion, spatio-temporal ICA.

I. INTRODUCTION

THE feasibility of contact-less measurements of vital signs renders new applications of medical-assistance systems inside daily routine applications possible. One promising technology is the capacitive electrocardiogram (cECG). In clinical routine, the standard ECG, i.e. ECG leads recorded by a set of electrodes attached to the skin, is an indispensable tool. From the ECG clinicians derive statements on the functioning of the heart by analyzing the heart rate, its variability and a couple of morphological characteristics (see an example for an ECG in Fig. 3/4: refECG). The cECG, in turn, has already been proven to measure accurately cardiovascular parameters like the heart rate (HR) within innovative measurement systems, e.g. integrated into a Chair back [3]. The integration of unobtrusive capacitively-coupled monitoring has also been extended to an automotive environment for screening purposes of drivers vigilance [12] and assessing the stress or health status of the driver [18]. Facing an automotive application Matsuda et al. focussed on technical aspects of a single-channel recording using a capacitively coupled electrode below subjects' buttocks and a conductive steering wheel during preliminary driving experiments. However, applying non-contact measurements (e.g. bringing in relative motion between driver and seat [18])

implies measurement instability which needs to be considered in designing said systems and applications.

Introducing redundancy by multichannel recordings can help to cope with arising problems at the expense of an increasing measurement complexity and requiring data fusion concepts. In this regard, Wartzek et al. proposed a solution for a multichannel cECG system by incorporating decision fusion (high-level fusion) to detect heart beats during driving experiments involving five subjects [18].

To overcome problems applying combinations of uncertain heart beat detections during recording phases of low signal-to-noise-ratio, our own approach to cope with the multichannel task is directed to raw data fusion (low-level-fusion) of capacitive ECGs. This concept is considered to provide the most accurate results under assumption of proper sensor association and alignment [5] which we can ensure easily. Relying on the assumption that observed measurements are mixtures of originally independent processes (e.g. cardiovascular activity and relative motion between driver and seat) one can apply independent component analysis (ICA) to decompose the observed signal mixtures [8]. While one can regard original ICA applied to simultaneously recorded ECG channels as pure spatial filtering, there exist several advancements to a spatio-temporal ICA capable of handling artefacts and disturbances during electrophysiological recordings [9], [13], [19]. The spatio-temporal filtering introduces a temporal dimension to the unmixing process by adding temporally delayed input signals [19]. The technique has previously been applied to different types of biosignals [14], [15], [19] and proved its capability to separate different components contained in multichannel recordings.

Despite of promising results regarding the decomposition by means of classical and spatio-temporal ICA algorithms, one obtains as many independent output signals as input signal mixtures which suffers from permutation indeterminacy [1]. Accordingly, the decomposition into its components requires the identification of the desired one afterwards to derive one statement, e.g. on the heart rate. Alternative solutions, directly extracting only a single output channel like deflational ICA [19] or targeting manipulation of ICA algorithm to a desired result (e.g. temporally constrained ICA (tICA) [10], [13]) have been proposed. Those solutions, however, go along with practical limitations. The general problem of deflational ICA arises from the morphological/statistical properties of artefacts which can mimic individual desired ECG characteristics. Single output ICAs whose selection typically relies on a single

D. Wedekind, H. Malberg and S. Zaunseder are with the Institute of Biomedical Engineering IBMT, Departement of Electrical Engineering, TU Dresden, Germany, e-mail: daniel.wedekind@tu-dresden.de

Manuscript received August 6th, 2013; revised September 29th, 2013

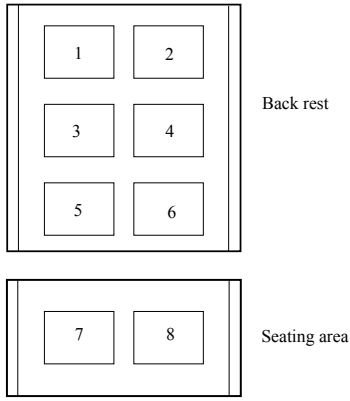


Fig. 1. Electrode arrangement on driver's seat (topview).

higher order statistical feature thus can easily get misled and produce an unwanted output. Further on, temporal features of the desired output signals as required for tICA are rarely available encountering an unobtrusive practical measurement environment.

Our work therefore aims at using multi-output ICA and combining it with a sophisticated method for a channel selection to detect heart beats from multichannel cECG. Different solutions for channel selection or exclusion have been outlined (frequency characteristics [17], statistics [4], [6], [17], [19], correlation [1], [13]). However, all suffer from specific drawbacks, most often from a low-dimensional feature space for the decision as described for deflational ICA.

To cope with the problem of automated channel selection in the context of cECG processing this contribution proposes a multivariate selection algorithm. Our cascaded output selection scheme targets two-step artefact exclusion following a best-channel-selection based on frequency characteristics of spatio-temporal ICA's output.

II. MATERIALS AND METHODS

A. Capacitive ECG System Description

Experimental data was recorded in a simulated driving environment incorporating a cECG system which has been integrated into a driver's seat. The capacitive system provided by capical Medical Solutions (<http://www.capical.de/>) comprises eight electrodes integrated into the seat cover. Two electrodes are situated in the seating area, the remaining six electrodes are arranged in the back rest (see Fig. 1). The system supplies seven capacitive ECG leads. Each of them constitutes a bipolar measurement between one of the electrodes and electrode three (the resulting leads are denominated corresponding to the first electrode, i.e. cECG1, cECG2, cECG4, ..., cECG8). Preliminary investigations have revealed that due to differing sizes and sitting positions the leads cECG5, cECG6, cECG7 show the most marked ECG characteristic. Hence, these leads are assumed to be the most suitable and are used exclusively in this study. Sampling frequency of the capacitive system was 500 Hz and data was preprocessed using a notch filter at 50 Hz before application of ICA.

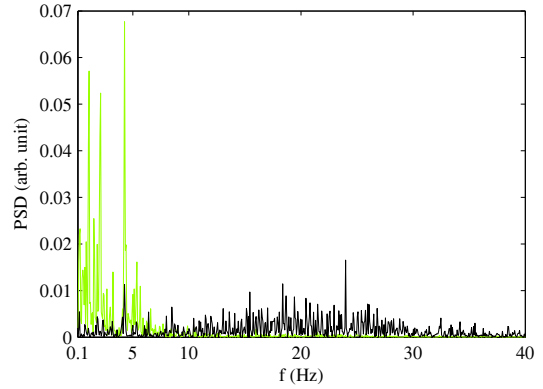


Fig. 2. Primary artefact rejection: PSD estimate of “usable” channel (black, see also Fig. 3: ICAex1) and an artefact channel (green, see also Fig. 3: ICAex2) after application of spatio-temporal ICA.

B. Experimental Protocol

27 healthy subjects (age 27.1 ± 4.8 years) performed an experimental protocol consisting of three measurement phases: rest, passive motion (movements introduced from outside the simulator) and active motion (typical driving movements resulting from instructed driving maneuvers). Each phase had duration of three minutes. In parallel to the capacitive measurement we recorded a standard ECG (modified Einthoven II lead) from which each single heart beat (and therewith the heart rate) was determined in a semi-automated manner (automated beat detections were corrected if necessary). That way a reference was established against which the results of the capacitive measurements are evaluated.

C. Spatio-temporal ICA

The observed cECG recordings are regarded as signal mixtures which consist of originally independent processes (e.g. cardiovascular activity, subject movement, measurement noise). In general, ICA solves the problem of finding the unknown mixing matrix by relying on the central limit theorem. The theorem states that the probability density function (PDF) of a signal mixture is always more gaussian than the PDF of its constituent source signals. ICA aims at maximizing non-gaussianity of the output signals [8], [19].

Raw data fusion is done using multi-channel spatio-temporal ICA following Wiklund et al. In [19] a pure spatial filtering using only the spatially distributed electrodes is supplemented by adding a temporal filtering dimension through constructing ICA input z as K time-delayed versions of each lead i according to

$$z_{i,k}(n) = x_i(n - k) \quad \text{for } k, i \in \mathbb{Z} \begin{cases} k \in [0, K - 1] \\ i \in [0, I - 1] \end{cases} \quad (1)$$

where $x_i(n)$ is the input signal from lead i . In this study the filter size was set to $K = 10$ samples and $I = 3$ (cECG5, cECG6, cECG7). The output of ICA is obtained by

$$y = Wz \quad (2)$$

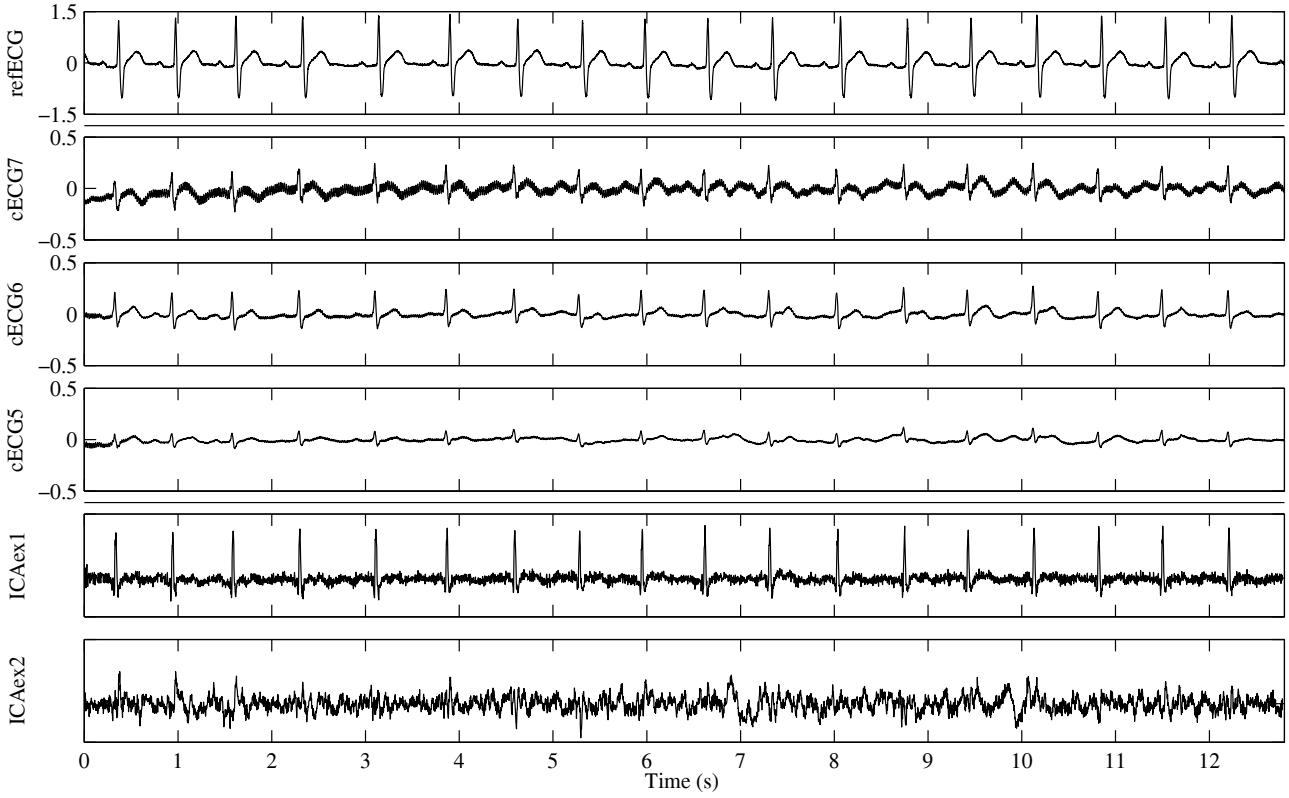


Fig. 3. Adaptive spatio-temporal filtering of a qualitatively “good” cECG recording during rest. *Top panel:* reference ECG (mV). *Middle panels:* cECG channels cECG5-cECG7 (mV). *Two bottom panels:* ICA output examples (arb. unit).

where \mathbf{W} is the quadratic $[I \cdot K \times I \cdot K]$ unmixing matrix. As a result, we obtain as many output as input channels (i.e. $N = 30$). The coefficients of \mathbf{W} are determined using FastICA [7] which includes whitening and maximizing skewness of the output. FastICA utilizes negentropy allowing an indirect and simple measurement of PDF features. Skewness thereby serves as measure of non-gaussianity of the ICA output. According to Wiklund et al., peaked signal shapes referred to as QRS complexes (see upper four panels inside Fig. 3), belonging to the ventricular depolarization inside the ECG and can be resembled through a spike train. A spike train forms a super-gaussian distribution with a marked tail in the histogram. This characteristic can be measured using skewness. Thus, maximizing skewness facilitates the unmixing of a disturbed ECG recording towards a spike train from which the heart rate can be derived.

Spatio-temporal ICA is performed on sliding windows of 12.8 s duration (window displacement 1.0 s). Thus adaptivity of ICA is achieved through consecutively updating the unmixing matrix \mathbf{W} [19].

D. Cascaded Output Channel Selection

The cascaded output selection is realized in three steps.

1) *Primary Output Channel Exclusion:* A primary artefact exclusion is implemented by calculating the ratio of high frequency (HF) power $P_{HF}^{(1)}$ and low frequency (LF) power $P_{LF}^{(1)}$ of each output channel. $P_{HF}^{(1)}$ and $P_{LF}^{(1)}$ are derived

from power spectral density (PSD) estimate which has been calculated using periodogram. A high HF-power is expected for usable channels as maximizing skewness can be obtained by strengthening waveforms belonging to QRS complexes. QRS complexes containing a marked high frequency content (up to 40 Hz [2], see Fig. 2 for an expected PSD behaviour after applying spatio-temporal ICA). Upper bound of investigated frequency range was set to 40 Hz. LF-power and HF-power are determined in the range of 0.1-5 Hz and 5-40 Hz, respectively. The 5 Hz bound was introduced to separate potentially desired output signals from low frequency powered noise. At that stage, output channels are regarded as usable if it holds $P_{HF}^{(1)}/P_{LF}^{(1)} \geq 1$.

2) *Secondary Output Channel Exclusion:* A secondary channel exclusion is performed after postprocessing of the remaining output channels from the first step. Application of a bandpass filter between 5-11 Hz, smoothed derivative filtering and squaring which is based on Pan and Tompkins QRS detection algorithm [16] aims at maximizing of QRS energy and reintroduces fundamental oscillations which are typically contained in an ECG (i.e. spectral peaks at the heart rate). An expected PSD-behaviour can be seen in Fig. 5 (black curve). Channels containing a relatively high LF-power are assumed to present desired waveforms. Consequently, power ratio estimation is performed on postprocessed channels by now estimating LF-power in the range of 0.5-5 Hz, which encloses a recommended range for heart rate monitoring [20] and ensures the inclusion of expected harmonic oscillations

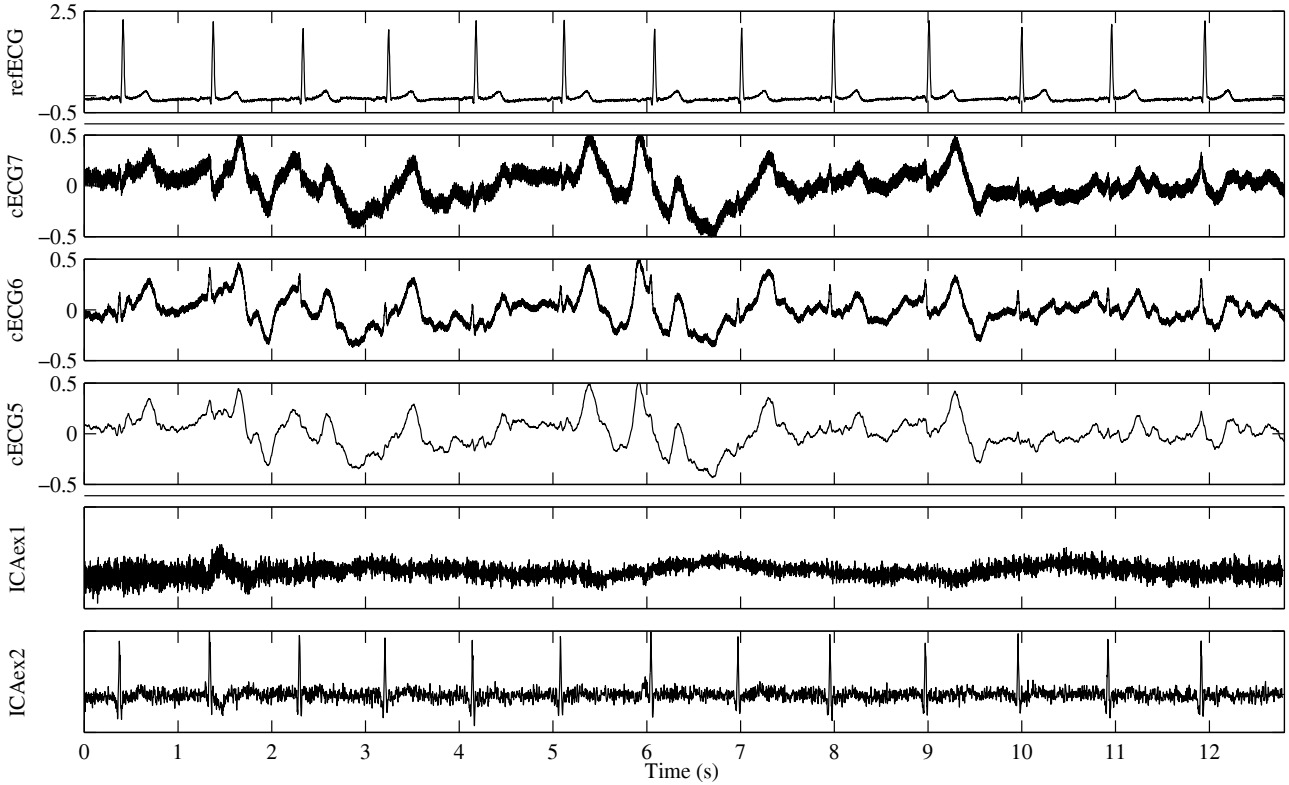


Fig. 4. Adaptive spatio-temporal filtering of a qualitatively “intermediate” cECG recording during rest. *Top panel:* reference ECG (mV). *Middle panels:* cECG channels cECG5-cECG7 (mV). *Two bottom panels:* ICA output examples (arb. unit).

of the heart rate inside PSD. HF-power is determined in the frequency range 5-30 Hz. A decreased upper frequency bound (30 Hz) compared to primary output channel exclusion is applicable due to limiting the high frequency content of the signals using the bandpass filter according to Pan and Tompkins. $P_{LF}^{(2)}/P_{HF}^{(2)} \geq d$ is used as criterion for a channel to be judged as usable. The initial threshold was set to $d = 1$ and allowed to decrease in the case of removing every remaining output channel with a given d .

3) *Best Channel Selection:* After removing corrupted channels, PSD (following postprocessing based on Pan and Tompkins) is used to choose the best channel among the remaining output channels. Assuming distinct fundamental and corresponding harmonic oscillations containing the heart rate inside frequency band 0.5-5 Hz of the desired signal (see also the black PSD inside Fig. 5), we estimate the root mean squared error (RMSE) referring to the median calculated of the PSD inside this frequency band. A desired PSD is expected to have a distinct deviation from its median inside the range of 0.5-5 Hz which contributes to a large RMSE. The channel with maximum RMSE is chosen to be the desired output.

E. Comparative Quality Assessment

To evaluate the algorithm, mean heart rates from the blocks of 12.8 s are compared to the reference heart rate derived from the standard ECG. The automated mean HR is obtained by applying the algorithm of Afonso et al. [2] to the found

“best” channel. Subsequently, the median for successive beat-to-beat intervals is used to determine the heart rate.

To assess the efficiency of our method, we compare our results to two alternative schemes to select the best channel as depicted by Wiklund et al.. On the one hand, channel selection using maximum skewness of the output is realized, as Wiklund applied for spatio-temporal ICA. On the other hand, Wiklund chose maximum kurtosis output to be considered as best channel for classical ICA [19].

In order to estimate an upper bound of achievable results by the best possible channel selection in addition we generate the

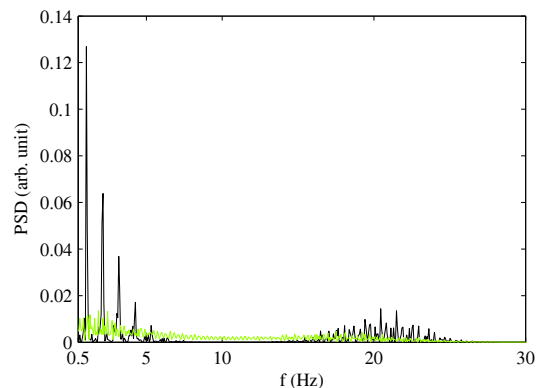


Fig. 5. Secondary artefact rejection: PSD estimate of “usable” channel (black, see also Fig. 4: ICAex2) and an artefact channel (green, see also Fig. 4: ICAex1) after filtering according to Pan and Tompkins.

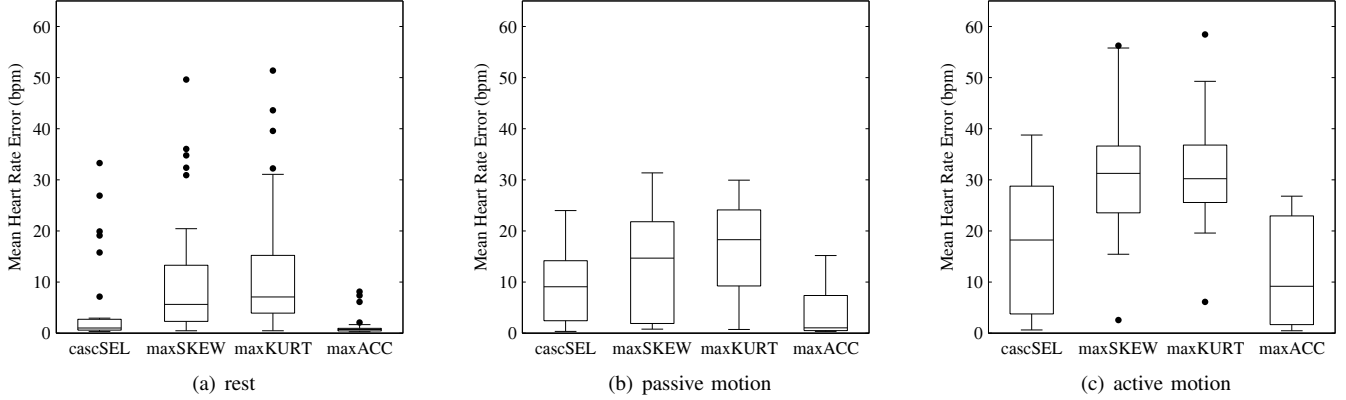


Fig. 6. Results for the measurement phases: rest, passive motion and active motion. Shown are comparative boxplots of mean heart rate errors (mHRE) realizing automated best channel selection according to cascaded output selection (cascSEL), maximum skewness output (maxSKEW), maximum kurtosis output (maxKURT) and maximum detection accuracy (maxACC) for all 27 subjects with outlier (●) definition as $|\text{mHRE}| > 1.5 \cdot \text{IQR}$ (with IQR as interquartile range).

theoretical optimum for the best channel selection involving the reference ECG. Considering automated detections [2] of every output channel, we estimate the QRS detection accuracy ACC (see [11]) compared to the reference ECG by

$$\text{ACC} = \frac{TP}{TP + FP + FN} \quad (3)$$

where TP are true positive, FP are false positive and FN are false negative detections. The output channel with maximum accuracy is chosen as optimal selection for the best channel from which the automated mean HR (maxACC) is derived for comparing to the algorithmic decision.

III. RESULTS

Fig. 3 and Fig. 4 show examples of the performance of spatio-temporal ICA with resting cECG excerpts of “good” and “intermediate” quality, respectively. Both figures show two exemplary channels (ICAex1, ICAex2) out of 30 available ICA output channels with different suitability. ICAex1 in Fig. 3 and ICAex2 in Fig. 4 represent the choices of our proposed best channel selection for the given signal excerpts.

Fig. 6 contains the averaged results of the mean heart rate error (mHRE) for the measurement phases rest, passive motion and active motion. Table I presents the corresponding means (mHRE) including median estimates of mHRE as well as means of the standard deviation of the mean heart rate error (stHRE). As can be seen, the proposed best channel

selection scheme using cascaded output channel selection works best in achieving minor mHRE compared to choosing one output channel with statistical properties skewness or kurtosis. Results comparable to the theoretical optimal channel selection maxACC (accepting mHRE differences < 1 bpm) are reached in 20 cases by comparing mHRE (cascSEL) during rest phase, in six cases during passive motion and seven cases during active motion (maxSKEW: 6/6/0, maxKURT: 3/5/0). Further on, initially starting from 30 ICA output channels, the artefact exclusion performance of the cascaded output selection achieves overall channel exclusion rates (mean \pm standard deviation) of 13.6 ± 7.5 excluded channels during primary artefact exclusion and 7.5 ± 4.6 excluded channels during secondary artefact exclusion, respectively.

IV. DISCUSSION

First of all it is worth noting that spatio-temporal ICA shows an eminent performance on extracting heart beat related spiky output channels out of rough disturbed cECG recordings (see Fig. 4 for an example). In-depth analysis of obtained output channels has shown the possibility of manually identifying at least one usable output channel in many cases. This underlines the worth and potential of a proper automated best channel selection for practical applications.

Further on, from distinctly increased mean mHRE compared to median mHRE (bracketed in Table I) during rest can be deduced that single outliers contribute heavily to the overall

TABLE I

MEANS (MEDIAN) OF MEAN HEART RATE ERRORS (mHRE) AND STANDARD DEVIATIONS (stHRE) [IN BPM] REALIZING AUTOMATED BEST CHANNEL SELECTION ACCORDING TO CASCADED OUTPUT SELECTION (CASCSEL), MAXIMUM SKEWNESS (MAXSKEW), MAXIMUM KURTOSIS (MAXKURT) AND MAXIMUM DETECTION ACCURACY (MAXACC) FOR ALL 27 SUBJECTS AND MEASUREMENT PHASES: REST, PASSIVE MOTION AND ACTIVE MOTION.

best channel selection measurement phase	cascSEL		maxSKEW		maxKURT		maxACC	
	mHRE	stHRE	mHRE	stHRE	mHRE	stHRE	mHRE	stHRE
rest	5.31 (0.99)	7.75	11.26 (5.63)	16.09	13.26 (7.06)	18.73	1.44 (0.70)	2.46
passive motion	9.33 (9.05)	14.63	13.74 (14.67)	18.03	16.14 (18.27)	20.70	3.99 (1.02)	6.35
active motion	18.58 (18.20)	19.53	30.94 (31.26)	29.30	31.76 (30.21)	29.78	12.10 (9.16)	13.72

error. Those outliers are owing to subjects' clothing (there were no specific requirement regarding clothing's material imposed to the participants). A degradation which can exclusively attributed to outliers doesn't hold during passive motion where overall performance is limited. The theoretical optimum (maxACC), however, highlights the possibility of further improvements of the channel selection. Active motion phase shows inadequate results, even considering theoretical optimum. Successfully handling of active motion probably will need more sophisticated approaches, maybe the integration of heterogeneous sensor fusion to overcome periods of poor cECG quality. The comparison between different methods of channel selection reveals that the proposed cascaded scheme consistently performs more accurately.

Addressing a distinction between a channel containing desired contents and a channel containing artefacts, we focus on frequency characteristics of desired cECG features at different processing stages (see Fig. 2 and 5). This approach differs from solutions as proposed for direct artefact exclusion (see [4], [6], [13]). Encountering several remaining output channels after two-step artefact exclusion, a best channel selection still needs to be realized. Investigations of interim results of the proposed channel selection scheme have proven that this processing step works weakest, i.e. it generates the main contribution to observed mHRE. The exclusion of unwanted channels (primary and secondary output channel exclusion) in contrast is working stable in terms of leaving at least one usable channel. An improved detection of desired signal contents hence needs to be further analyzed.

Moreover, in case of artefact retention inside simultaneous usable output channels, coexisting artefacts and desired heart beats in the same channel complicate automated heart beat detection. This could be observed e.g. in case of missing convergence during FastICA algorithm thereby contributing to mHRE as well as to the theoretically achievable optimum.

Nevertheless, we showed in this contribution that the proposed cascaded output selection scheme works best (see also Table I) compared to channel selections using higher order statistics [19]. Considering maxSKEW and maxKURT we observed that the main contribution of degraded results arises from high energetic artefacts. Secure artefact exclusion before using skewness/kurtosis for selecting the best output channel is therefore assumed to potentially overcome this problem.

V. CONCLUSION

Our primary goal was to develop and evaluate an automated best channel selection scheme for choosing an adequate output channel out of several ($N = 30$) output channels which have been obtained by applying spatio-temporal ICA as multi-output algorithm. For this purpose, a two-step channel exclusion was realized to reduce the initial amount of output channels to a count of probably usable channels followed by a "best" channel selection. The selected channel was then evaluated by calculating mean heart rates errors of consecutive blocks for different experimental conditions and regarding a reference ECG.

Our work shows that relying on some desired frequency characteristics enables successful handling channel selection

after spatio-temporal ICA in many cases of rough disturbed cECG recordings. The main benefit results from the usage of complete multi-output information thereby initially avoiding the exclusion of desired outputs of the ICA algorithm.

More detailed classification of favored cardiovascular content inside electrocardiographic signals will contribute to further improve the results of the channel selection in the future.

REFERENCES

- [1] A. Acharyya, K. Maharatna, B.M. Al-Hashimi and S. Mondal, *Robust channel identification scheme: solving permutation indeterminacy of ICA for artifacts removal from ECG*, in Proceedings of the 32nd Annual International Conference of the IEEE Engineering in Medicine and Biology Society, Buenos Aires, Argentina, 2010, pp. 1142-1145.
- [2] V. Afonso, W. Tompkins, T. Nguyen and S. Luo, *ECG Beat Detection Using Filter Banks*, IEEE Trans. Biomed. Eng., vol. 46, no. 2, pp. 192-202, 1999.
- [3] M. Czaplik, B. Eilebrecht, R. Walocha, M. Walter, P. Schauerer, S. Leonhardt and R. Rossaint, *The Reliability and Accuracy of a Noncontact Electrocardiograph System for Screening Purposes*, Anesth. Analg., vol. 114, no. 2, pp. 322-327, 2012.
- [4] A. Delorme, T. Sejnowski and S. Makeig, *Enhanced detection of artifacts in EEG data using higher-order statistics and independent component analysis*, Neuroimage, vol. 34, no. 4, pp. 1443-1449, 2007.
- [5] D. Hall and J. Llinas *An Introduction to Multisensor Data Fusion*, IEEE J. Proc., vol. 85, no. 1, pp. 6-23, 1997.
- [6] T. He, G. Clifford and L. Tarassenko *Application of independent component analysis in removing artefacts from the electrocardiogram*, Neural Comput. Applic., vol. 15, no. 2, pp. 105-116, 2006.
- [7] A. Hyvärinen, *Fast and Robust Fixed-Point Algorithms for Independent Component Analysis*, IEEE Trans. Neural Netw., vol. 10, no. 3, pp. 626-634, 1999.
- [8] A. Hyvärinen, *Independent component analysis: recent advances*, Phil. Trans. R. Soc. A, vol. 371, no. 1984, pp. 1-19, 2013.
- [9] C. James and D. Lowe, *Extracting multisource brain activity from a single electromagnetic channel*, Artif. Intell. Med., vol. 28, no. 1, pp. 89-104, 2003.
- [10] C. James and O. Gibson, *Temporally Constrained ICA: An Application to Artifact Rejection in Electromagnetic Brain Signal Analysis*, IEEE Trans. Biomed. Eng., vol. 50, no. 9, pp. 1108-1116, 2003.
- [11] E. Karvounis, M. Tsipouras, D. Fotiadis and K. Naka, *An automated methodology for fetal heart rate extraction from the abdominal electrocardiogram.*, IEEE Trans. Inf. Technol. Biomed., vol. 11, no. 6, pp. 628-638, 2007.
- [12] T. Matsuda and M. Makikawa, *ECG Monitoring of a Car Driver Using Capacitively-Coupled Electrodes*, in Proceedings of the IEEE Engineering in Medicine and Biology 30th Annual Conference, Vancouver, Canada, 2008, pp. 1315-1318.
- [13] M. Milanese, N. Martini and N. Vanello, *Independent component analysis applied to the removal of motion artifacts from electrocardiographic signals*, Med. Biol. Eng. Comput., vol. 46, no. 3, pp. 251-261, 2008.
- [14] N. Östlund, U. Wiklund, J. Yu and J.S. Karlsson, *Adaptive spatio-temporal filtration of bioelectrical signals*, in Proceedings of the IEEE Engineering in Medicine and Biology 27th Annual Conference, Shanghai, China, 2005, pp. 5983-5986.
- [15] N. Östlund, J. Yu and J.F. Karlsson, *Adaptive spatio-temporal filtering of multichannel surface EMG signals*, Med. Biol. Eng. Comput., vol. 44, no. 3, pp. 209-215, 2006.
- [16] J. Pan and W. Tompkins, *A Real-Time QRS Detection Algorithm*, IEEE Trans. Biomed. Eng., vol. 32, no. 3, pp. 230-236, 1985.
- [17] J. Rieta, F. Castells, C. Sánchez, V. Zarzoso and J. Millet, *Atrial Activity Extraction for Fibrillation Analysis Using Blind Source Separation*, IEEE Trans. Biomed. Eng., vol. 51, no. 7, pp. 1176-1186, 2004.
- [18] T. Wartzek, B. Eilebrecht, J. Lem, H.J. Lindner, S. Leonhardt and M. Walter, *ECG on the Road: Robust and Unobstrusive Estimation of Heart Rate*, IEEE Trans. Biomed. Eng., vol. 58, no. 11, pp. 3112-3120, 2011.
- [19] U. Wiklund, M. Karlsson, N. Östlund, L. Berglin, K. Lindcrantz, S. Karlsson and L. Sandsjö, *Adaptive spatio-temporal filtering of disturbed ECGs: a multi-channel approach to heartbeat detection in smart clothing*, Med. Biol. Eng. Comput., vol. 45, no. 6, pp. 515-523, 2007.
- [20] *Cardiac monitors, heart rate meters, and alarms*, ANSI Standard EC13:2002.